FoxO1 Haploinsufficiency Protects Against High-Fat Diet–Induced Insulin Resistance With Enhanced Peroxisome Proliferator–Activated Receptor γ Activation in Adipose Tissue

Jane J. Kim,[1,2] Pingping Li,[3] Jessica Huntley,[1] Jeffrey P. Chang,[1] Karen C. Arden,[3,4] and Jerrold M. Olefsky[3]

OBJECTIVE—Forkhead box O (FoxO) transcription factors represent evolutionarily conserved targets of insulin signaling, regulating metabolism and cellular differentiation in response to changes in nutrient availability. Although the FoxO1 isoform is known to play a key role in adipogenesis, its physiological role in differentiated adipose tissue remains unclear.

RESEARCH DESIGN AND METHODS—In this study, we analyzed the phenotype of FoxO1 haploinsufficient mice to investigate the role of FoxO1 in high-fat diet–induced obesity and adipose tissue metabolism.

RESULTS—We showed that reduced FoxO1 expression protects mice against obesity-related insulin resistance with marked improvement not only in hepatic insulin sensitivity but also in skeletal muscle insulin action. FoxO1 haploinsufficiency also resulted in increased peroxisome proliferator–activated receptor (PPAR)γ gene expression in adipose tissue, with enhanced expression of PPARγ target genes known to influence metabolism. Moreover, treatment of mice with the PPARγ agonist rosiglitazone caused a greater improvement in in vivo insulin sensitivity in FoxO1 haploinsufficient animals, including reductions in circulating proinflammatory cytokines.

CONCLUSIONS—These findings indicate that FoxO1 proteins negatively regulate insulin action and that their effect may be explained, at least in part, by inhibition of PPARγ function. ***Diabetes*** **58:1275–1282, 2009**

Adipose tissue is the body's largest endocrine organ, representing a complex, essential, and highly active metabolic site of insulin action. Moreover, excess adiposity, or obesity, is associated with insulin resistance, hyperglycemia, dyslipidemia, and hypertension. Deciphering how vertebrates integrate both intracellular and extracellular cues to regulate metabolism in adipose tissue may be central to understanding the metabolic complications associated with obesity.

The O subfamily of forkhead box (Fox) transcription factors are direct targets of insulin action, regulating cellular metabolism and survival in response to nutrient and environmental stress. In addition, FoxO proteins appear to play pivotal roles in the transcriptional cascades that control differentiation in preadipocytes, myoblasts, and endothelial cells (1). FoxO1 represents the predominant FoxO isoform present in both white and brown adipose tissue. In preadipocytes, FoxO1 expression occurs before the expression of peroxisome proliferator–activated receptor (PPAR)γ, and tight temporal regulation of its activity is required for differentiation to proceed. For example, ectopic nuclear expression of FoxO1 via transduction of constitutively active FoxO1 mutants results in the inhibition of adipogenesis (2). Although complete FoxO1 ablation causes embryonic lethality in vivo, FoxO1 haploinsufficiency yields viable offspring and restores normal insulin sensitivity in genetic models of insulin resistance (3). In addition, FoxO1 haploinsufficiency has been reported to reduce cell size and increase cell numbers of adipocytes under a high-fat diet (HFD) (2). However, little is known regarding the physiological role of FoxO1 in fully differentiated adipose tissue.

The PPARγ nuclear receptor plays a crucial role in adipocyte metabolism and survival (4). Activation of PPARγ in the early phases of adipogenesis is well characterized and is considered an absolute requirement for adipocyte differentiation, controlling the subsequent expression of adipocyte-specific genes involved in lipid storage and metabolic control. The antidiabetes thiazolidinedione (TZD) drugs have been identified as synthetic ligands of PPARγ, exerting potent effects to improve insulin action (4). PPARγ activation in peripheral tissues is now established as a well-recognized approach to enhance insulin sensitivity, although the mechanism of action is only partially understood (5).

The convergence of FoxO1 and PPARγ signaling pathways may represent an important mechanism regulating energy homeostasis and insulin sensitivity in obesity. Their differing roles in adipogenesis (2,4) suggest that these two transcription factors also possess opposing roles in the metabolic control of mature adipocytes as well. We, therefore, hypothesized that FoxO1 might hamper PPARγ activity and that inhibition of FoxO1 may lead to improved insulin sensitivity, particularly in response to treatment with PPARγ ligand. To date, only a few precedents for the convergence of FoxO1 and PPARγ exist in mammalian systems (6,7), and no studies have yet shown

From the [1]Department of Pediatrics, University of California at San Diego, La Jolla, California; [2]Rady Children's Hospital of San Diego, San Diego, California; the [3]Department of Medicine, University of California at San Diego, La Jolla, California; and the [4]Ludwig Institute for Cancer Research, University of California at San Diego, La Jolla, California.
Corresponding author: Jane J. Kim, janekim@ucsd.edu.
Received 23 July 2008 and accepted 3 March 2009.
Published ahead of print at http://diabetes.diabetesjournals.org on 16 March 2009. DOI: 10.2337/db08-1001.

their interaction in vivo. In this study, we demonstrate that FoxO1 haploinsufficiency leads to a reduction in insulin resistance induced by HFD, with improvements in PPARγ expression and activity.

RESEARCH DESIGN AND METHODS

Mutant mice. Generation of the targeted *Foxo1* allele has been described (8). Because the homozygous FoxO1 deletion is embryonic lethal, only heterozygous mice were used. Male mice (aged 4 months) were fed a HFD for 4–24 weeks with 45% kcal from fat (Harlan Teklad Custom Diets). Mice treated with TZD were fed rosiglitazone (3 g/day) blended into the same HFD. All mice were maintained on a C57BL/6 background, and wild-type littermates were used as controls. All mouse procedures conformed to the *Guide for Care and Use of Laboratory Animals* of the National Institutes of Health and were approved by the Animal Subjects Committee of the University of California, San Diego.

Phenotypic evaluation of mice. We studied male *Foxo1*$^{+/-}$ and wild-type mice, with or without TZD treatment (3 mg · kg^{-1} · day^{-1} rosiglitazone). Body weight measurements were obtained weekly. Whole blood was collected, and the plasma was withdrawn for subsequent analysis of glucose, insulin, and free fatty acids (FFAs). Plasma cytokines were measured by the core laboratories of the Diabetes and Endocrinology Research Consortium (University of California, Los Angeles, CA).

Glucose and insulin tolerance tests. Mice were fasted for 6 h, followed by injection with dextrose (1 g/kg) or regular human insulin (0.35 unit/kg) into the peritoneal cavity. Blood samples were drawn by tail vein sampling at 0, 15, 30, 60, 90, and 120 min for glucose and/or insulin measurement.

Hyperinsulinemic-euglycemic clamp studies. In two separate groups of mice, aged 5 and 10 months, animals were implanted with two catheters that were tunneled subcutaneously, exteriorized at the back of the neck, and encased in Silastic tubing. Four days after surgery, animals were fasted for 6 h, and clamp studies were performed. A basal blood sample was taken at −90 min and measured for glucose, insulin, and FFA levels. After this, a primed constant infusion of 5.0 μCi/h (0.12 ml/h) of [3-^{3}H]D-glucose (NEN Life Science Products) was initiated. At time 0, a basal blood sample was drawn for determination of glucose-specific activity. After basal sampling, glucose (50% dextrose) and insulin (12 mU · kg^{-1} · min^{-1}) plus tracer (5.0 μCi/h) infusions were initiated simultaneously, and glucose levels were clamped at euglycemia using a variable glucose infusion rate (GIR). Steady state was achieved when blood glucose was successfully clamped, and the GIR was fixed for a minimum of 30 min. At the end of the clamp, a final blood sample was taken for the determination of tracer-specific activity. The insulin-stimulated glucose disposal rate (IS-GDR) is equal to the total glucose disposal rate minus the basal glucose turnover rate.

mRNA isolation and RT-PCR. mRNA was isolated using an RNeasy Mini Kit (Qiagen). We reverse-transcribed RNA using a High Capacity cDNA Reverse Transcription kit (Applied Biosystems) and then performed real-time PCR using an ABI 7300 system. Each reaction was measured in duplicate under standard reaction conditions. SYBR Green oligonucleotides were used for detection and quantification of a given gene, expressed as the mRNA level normalized to a standard housekeeping gene (glyceraldehyde-3-phosphate dehydrogenase [GAPDH] or β-actin) using the $\Delta\Delta C_T$ method. We performed separate control experiments to ensure that the efficiencies of target and reference amplification were equal. The specificity of the PCR amplification was verified by melting curve analysis of the final products using Opticon 3 software (Bio-Rad). Primer sequences used to amplify *Pparγ*, *Pck1*, *Pdk4*, *Sorbs1*, *Glut4*, *F4/80*, *CD11c*, *GAPDH*, and *β-actin* are available upon request.

Histochemistry. Paraffin-embedded adipose tissue sections were stained with MAC2 (Cedarlane Laboratories). Stained slides were subsequently coverslipped with 4,6-diamidino-2-phenylindole-containing mounting medium (Vector Laboratories). Adipocyte size and percentage of MAC2-positive crown-like structures per field were calculated as described previously (9,10).

Programmed array plate analysis. The array plate mRNA assay combined a multiplexed nuclease protection assay with array detection, performed by high-throughput genomics (11). Liver tissue homogenates were first lysed in the presence of probes binding target mRNA species. Upon addition of S1 nuclease, excess probes and unhybridized mRNA were degraded, such that only mRNA:probe duplexes remained. Alkaline hydrolysis destroyed the mRNA component of the duplexes, leaving probes intact. After the addition of neutralization solution, the probes were transferred to a programmed array plate containing a 16-element array at the bottom of each well. Each array element comprised a position-specific anchor oligonucleotide. The binding specificity of each of the 16 anchors was modified with a programming linker oligonucleotide complementary at one end to an anchor and at the other end to a nuclease protection probe. During a hybridization reaction, probes were captured by an immobilized programming linker and then were labeled with a detection linker oligonucleotide, which was in turn labeled with a detection conjugate that incorporated peroxidase. Chemiluminescent substrate was applied, and the enzyme-produced light was captured in a digital image. The light intensity at each array element was used as a measure of the target mRNA present in the original tissue lysate.

Immunoblotting. We carried out immunoblotting on liver, muscle, and adipose tissues collected from fasted mice. After animals were anesthetized by the intraperitoneal administration of a ketamine-xylazine-acepromazine cocktail, the right epididymal fat pad and right hindlimb (gastrocnemius and quadriceps) muscles were removed. Regular insulin (10 units/kg) was then injected through the inferior vena cava, and sections of the liver and left hindlimb muscles were taken at 1 and 3 min after insulin injection, respectively. To measure Akt phosphorylation, solubilized extracts containing equal amounts of tissue protein were immunoblotted with rabbit polyclonal antibodies against either Akt or phospho-Ser^{473} Akt (Cell Signaling Technology, Beverly, MA), followed by second antibody detection. Immunoblots were analyzed by densitometry, and the results expressed as arbitrary units.

Statistical analyses. All values are expressed as means ± SE unless otherwise noted. We used ANOVA to determine differences between groups, and repeated-measures ANOVA testing for comparisons over time. $P < 0.05$ was considered significant.

RESULTS

FoxO1 haploinsufficient mice are protected from HFD-induced insulin resistance. To investigate the functional role of FoxO1 in HFD-induced obesity, *Foxo1*$^{+/-}$ and wild-type mice (4 months old) were fed a 45% HFD for 24–28 weeks. Whole-body weights did not differ between *Foxo1*$^{+/-}$ mice and their wild-type littermates (Table 1). Previous studies have shown no differences in glucose or insulin homeostasis between wild-type and *Foxo1*$^{+/-}$ mice fed a normal chow diet (2).

FoxO1 haploinsufficient mice exhibited a striking age-related phenotype, developing enhanced insulin sensitivity after 24 weeks of the HFD. Although we performed intraperitoneal glucose and insulin tolerance tests every 4 weeks after initiation of the HFD, no significant differences between genotypes emerged until 24 weeks. At this point, *Foxo1*$^{+/-}$ mice demonstrated lower fasting blood glucose (*Foxo1*$^{+/-}$ 160 ± 5.2 mg/dl vs. wild type 193 ± 9.6 mg/dl, $P < 0.01$) and plasma insulin levels (*Foxo1*$^{+/-}$ 4.27 ± 0.6 vs. wild type 8.11 ± 1.7 mg/dl, $P < 0.05$). Accordingly, improved insulin sensitivity was observed in *Foxo1*$^{+/-}$ mice in glucose tolerance tests, as evident by reduced postabsorptive glucose and insulin values (Fig. 1*A* and *B*). Consistent with these results, the glucose-lowering effects of insulin were significantly enhanced in HFD-fed *Foxo1*$^{+/-}$ mice during insulin tolerance tests (Fig. 1*C* and *D*). No differences in body weight were detected between the two groups (Fig. 1*E*). Together, these data indicate an age-dependent protection from HFD-induced insulin resistance in *Foxo1*$^{+/-}$ mice, similar to previous published reports (2).

Insulin sensitivity is enhanced in both liver and skeletal muscle of FoxO1 haploinsufficient mice. We next examined tissue-specific insulin action by conducting hyperinsulinemic-euglycemic clamp experiments at 10 months of age after 26 weeks of the HFD. These studies further supported our glucose tolerance test (GTT) and insulin tolerance test (ITT) findings with an almost twofold increase in the glucose infusion rate in *Foxo1*$^{+/-}$ mice compared with controls (*Foxo1*$^{+/-}$ 48.6 ± 7.9 vs. wild type 26.0 ± 5.9 mg · kg^{-1} · min^{-1}, $P < 0.05$) (Fig. 2*A* and supplementary Fig. 1, available in an online appendix at http://diabetes.diabetesjournals.org/cgi/content/full/db08-1001/DC1). *Foxo1*$^{+/-}$ mice also demonstrated significantly lower rates of basal hepatic glucose output (*Foxo1*$^{+/-}$

TABLE 1
Characteristics of *Foxo1*$^{+/-}$ mice fed a HFD ± TZD

	HFD			HFD + TZD		
	Wild type	*Foxo1*$^{+/-}$	*P*	Wild type	*Foxo1*$^{+/-}$	*P*
n	10	14		5	6	
Age (months)	10	10		5	5	
Duration of diet (weeks)	24	24		5	5	
Body weight (g)	41.8 ± 0.9	41.6 ± 1.0	NS	35.8 ± 0.9	34.5 ± 0.9	NS
Fasting blood glucose (mg/dl)	193 ± 9.6	160 ± 5.2	0.01	175 ± 8.6	140 ± 8.1	0.02
Fasting plasma insulin (mg/dl)	8.11 ± 1.7	4.27 ± 0.6	0.05	1.43 ± 0.17	0.95 ± 12	0.05
Fasting free fatty acids (mmol/l)	0.56 ± 0.04	0.59 ± 0.05	NS	0.54 ± 0.03	0.54 ± 0.03	NS
Plasma adiponectin (ng/ml)	6,827 ± 415	5,318 ± 372	0.03	10,329 ± 1,386	11,425 ± 2,066	NS
Plasma leptin (pg/ml)	16,059 ± 2,382	14,320 ± 605	NS	11,631 ± 1,898	8,016 ± 1,682	NS
Plasma monocyte chemoattractant protein-1 (pg/ml)	46.4 ± 4.9	61.4 ± 7.1	NS	39.9 ± 10.5	21.1 ± 5.8	NS
Plasma interleukin-6 (pg/ml)	17.4 ± 2.4	11.4 ± 1.7	0.05	9.8 ± 5.6	4.2 ± 0.6	NS
Plasma tumor necrosis factor-α (pg/ml)	4.2 ± 0.4	4.9 ± 0.8	NS	3.0 ± 0.5	5.3 ± 0.5	0.01
Liver weight (g)	2.92 ± 0.31	2.35 ± 0.17	0.05	1.96 ± 0.09	2.01 ± 0.09	NS
Epididymal fat mass (g)	2.41 ± 0.32	3.17 ± 0.34	0.03	1.74 ± 0.09	1.41 ± 0.11	0.03
Liver triglyceride content (mg/g)	2.20 ± 0.53	1.87 ± 0.23	NS	1.48 ± 0.40	1.36 ± 0.23	NS
Adipocyte cell size (arbitrary units)	8,688 ± 626	6,426 ± 633	0.03	4,880 ± 224	7,630 ± 813	0.03

5.94 ± 1.93 vs. wild type 11.82 ± 1.95 mg · kg^{-1} · min^{-1}) as well as markedly improved insulin-stimulated suppression of hepatic glucose output (*Foxo1*$^{+/-}$ 71.2 ± 9.2 vs. wild type 32.3 ± 3.8%, $P < 0.05$) (Fig. 2*B*). These data are consistent with changes in gluconeogenic gene expression shown previously after dominant-negative FoxO1 inactivation in hepatocytes (12–14). Skeletal muscle is the major site of glucose uptake, and, interestingly, we observed a marked improvement in skeletal muscle insulin sensitivity of *Foxo1*$^{+/-}$ mice, as shown by 1.5- and 2-fold increases in

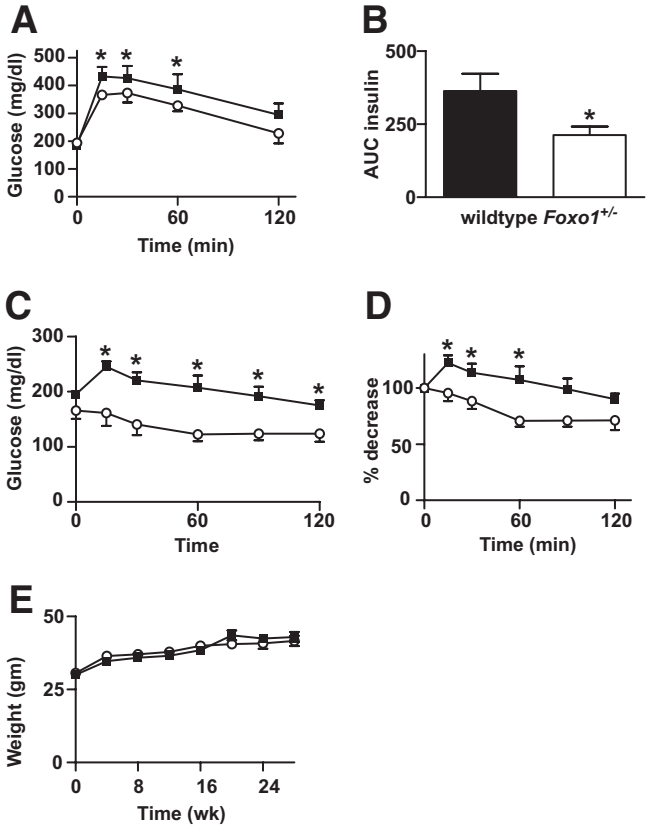

FIG. 1. Metabolic characterization of HFD-fed *Foxo1*$^{+/-}$ mice. Metabolic features of 10-month-old male mice after 24 weeks of a HFD (wild type $n = 10$; *Foxo1*$^{+/-}$ $n = 14$). *A* and *B*: Whole-blood glucose and plasma insulin during intraperitoneal glucose tolerance testing. *C* and *D*: Insulin tolerance testing. Animals were fasted for 6 and 4 h before GTTs and ITTs, respectively. Results are represented as both absolute glucose values and percent glucose decrease from basal. Values represent mean glucose ± SE. *$P < 0.05$ for *Foxo1*$^{+/-}$ versus wild-type. *E*: Mice were weighed at the initiation of the HFD and then at 4-week intervals up to 28 weeks of HFD duration. Values represent mean body weight of at least 15 mice per genotype ± SE. ■, wild type; ○, *Foxo1*$^{+/-}$.

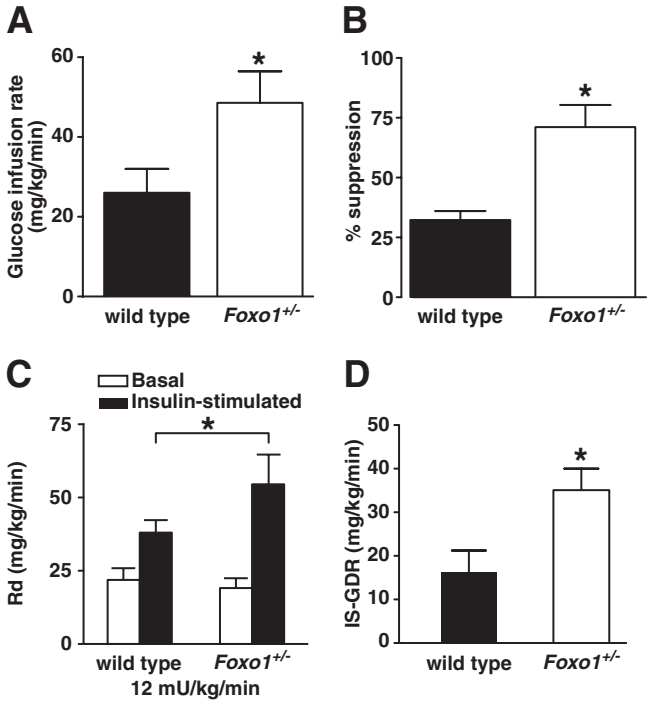

FIG. 2. Improved liver and skeletal muscle insulin sensitivity in *Foxo1*$^{+/-}$ mice. Hyperinsulinemic-euglycemic clamp studies were performed in 10-month-old male mice after 26 weeks of a HFD (wild type $n = 4$; *Foxo1*$^{+/-}$ $n = 5$). *Foxo1*$^{+/-}$ mice show increased GIRs. *A*: Decreased basal hepatic glucose output (*Foxo1*$^{+/-}$ 5.94 ± 1.93 vs. wild type 11.82 ± 1.95 mg/kg/min, $P < 0.05$) and improved insulin-stimulated hepatic glucose suppression (*B*) when compared with wild-type littermates. *Foxo1*$^{+/-}$ mice also demonstrate enhanced total Rd (*C*) and IS-GDR (*D*). Values represent the means ± SE. *$P < 0.05$.

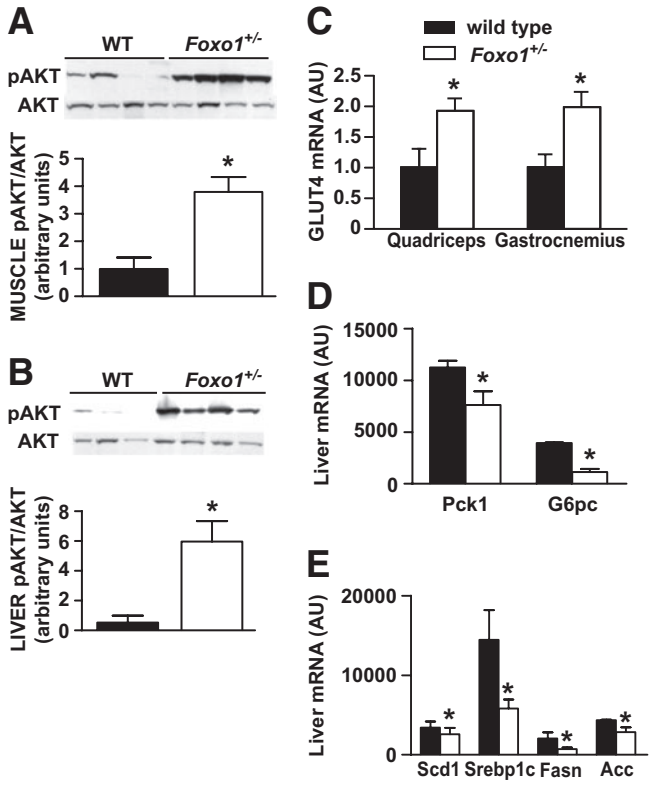

FIG. 3. Insulin action in liver and muscle of *Foxo1*$^{+/-}$ mice. *A* and *B*: Enhanced signaling through the PI3K pathway in *Foxo1*$^{+/-}$ and wild-type (WT) mice was determined by measuring Akt activity after insulin injection into the inferior vena cava. Representative blots from quadriceps muscle and liver are shown. The intensity of bands corresponding to phospho-Akt (pAkt) was corrected by total Akt levels to obtain relative measures of Akt phosphorylation between samples. Quantitation of results from three independent experiments is shown. *C*: Glut4 gene expression in skeletal muscle. Relative mRNA amounts of Glut4 from quadriceps and gastrocnemius muscle of HFD-fed *Foxo1*$^{+/-}$ and wild-type mice were measured using real-time PCR. *D* and *E*: Liver gene expression analysis. Relative mRNA amounts of genes controlling gluconeogenesis and lipogenesis were measured in fasted mice using a 16-gene microarray platform (wild type $n = 4$; *Foxo1*$^{+/-}$ $n = 6$). Values represent the means ± SE. *$P < 0.05$. The same cohort of HFD-fed *Foxo1*$^{+/-}$ and wild-type mice was used for all of the above experiments. RNA samples were isolated from fasting mice before insulin injection. AU, arbitrary units.

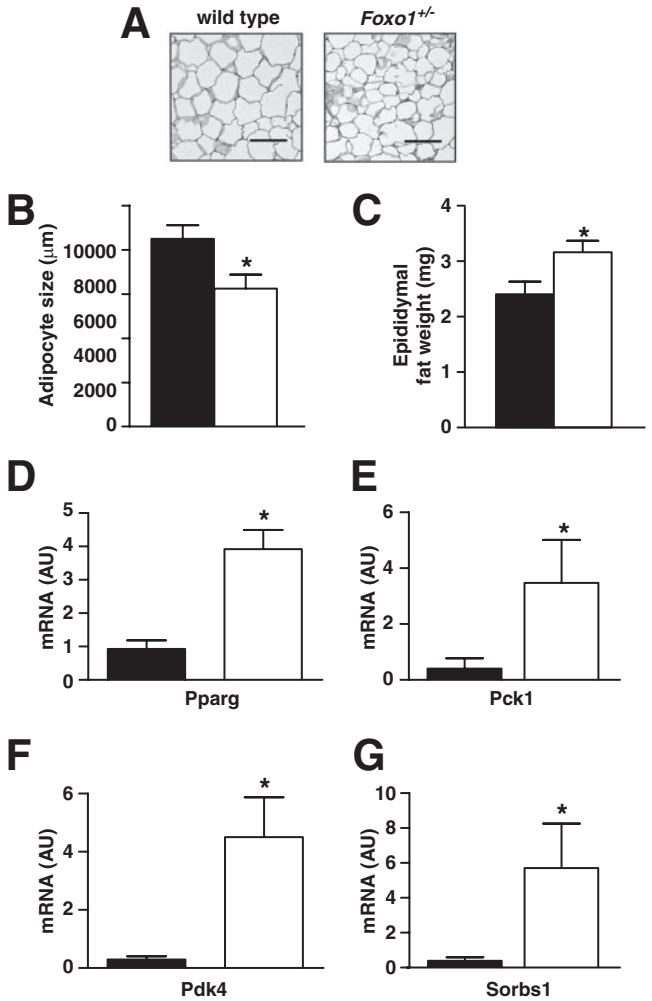

FIG. 4. Adipose tissue characteristics of HFD-fed *Foxo1*$^{+/-}$ mice. *A* and *B*: Average cell size of adipocytes from epididymal fat (wild type $n = 6$; *Foxo1*$^{+/-}$ $n = 8$). Representative photomicrographs are represented. Scale bars represent 100 μm. *C*: Epididymal adipose fat pads were isolated and weighed in HFD-fed wild-type and *Foxo1*$^{+/-}$ mice. Each bar represents individual means ± SE. *$P < 0.03$. *D–G*: Gene expression studies were performed on white adipose tissue of HFD-fed animals using real-time PCR to measure relative amounts of PPARγ and PPARγ target genes. Data represent means ± SE of RNA samples ($n = 5$ mice per genotype). *$P < 0.05$. AU, arbitrary units. ■, wild type; □, *Foxo1*$^{+/-}$.

total glucose turnover (Fig. 2*C*) and IS-GDRs (Fig. 2*D*), respectively, compared with wild-type controls.

Consistent with the improved insulin sensitivity found in the clamp studies, Akt phosphorylation was significantly enhanced by fourfold in muscle and sixfold in liver of *Foxo1*$^{+/-}$ mice after insulin stimulation (Fig. 3*A* and *B*). We found no differences in the phosphorylation of the insulin receptor, insulin receptor substrate (IRS)-1 or IRS-2 (data not shown). Subsequent measurements of Glut4 gene expression in skeletal muscle demonstrated a significant increase in Glut4 mRNA in both gastrocnemius (1.98-fold increase, $P \leq 0.05$) and quadriceps muscle (1.92-fold increase, $P = 0.02$) of HFD-fed *Foxo1*$^{+/-}$ mice, consistent with the enhanced glucose disposal observed during the clamp experiments (Fig. 3*C*).

To further investigate the FoxO1-mediated improvement in hepatic insulin sensitivity, we used a 16-gene microarray to measure the expression of liver genes. As expected, gluconeogenic gene expression (*Pck1* and *G6pc*) was reduced in *Foxo1*$^{+/-}$ mice (Fig. 3*D*). In addition, we observed a decrease in the expression of genes known to regulate lipogenesis (*Scd1*, *Srebp1c*, *Fasn*, and *Acc*) (Fig. 3*E*) after a 6-h fast. Although liver triglyceride content appeared to be lower in *Foxo1*$^{+/-}$ mice (*Foxo1*$^{+/-}$ 1.87 ± 0.23 vs. wild type 2.20 ± 0.53 mg · dl^{-1} · mg liver tissue^{-1}), this difference did not reach statistical significance. Plasma FFA levels were similar between genotypes (data not shown).

FoxO1 haploinsufficiency affects PPARγ activation in white adipose tissue. FoxO1 is highly expressed in preadipoctyes and is known to regulate adipocyte differentiation. Of note, dominant-negative FoxO1 expression promotes adipogenesis in insulin-receptor–deficient cells (2). FoxO1 has also been reported to regulate target genes involved in apoptosis, cell cycle regulation, stress resistance, and DNA repair. Histological analysis of epididymal fat revealed that adipocyte cell size was significantly smaller in *Foxo1*$^{+/-}$ mice (Fig. 4*A* and *B* and supplementary Fig. 2, available in an online appendix), similar to previous reports (2). However, epididymal fat pad weights were 31% higher in the knockout mice (Fig. 4*C*) despite similar body weights of HFD-fed *Foxo1*$^{+/-}$ and wild-type

mice, suggesting a role for FoxO1 in the development of this adipose depot. FoxO1 has been shown to upregulate mouse adiponectin gene expression by forming a transcriptional complex with CCAAT/enhancer-binding protein α and binding to the adiponectin promoter in differentiated adipocytes (15). Interestingly, plasma adiponectin levels were 22% lower in FoxO1 haploinsufficient mice (Table 1), perhaps due to reduced FoxO1 binding at the adiponectin promoter. Plasma leptin and free fatty acid levels were unchanged (data not shown). Plasma interleukin (IL)-6 levels were 35% lower in *Foxo1*$^{+/-}$ mice (Table 1), but macrophage content did not differ based on F4/80 staining of histological sections of adipose tissue (data not shown).

Recent in vitro studies from our group and others demonstrate that the FoxO1 transcription factor negatively regulates PPARγ promoter activity in cultured mammalian cells (6,7,16). Interestingly, we found that *Pparg* mRNA expression levels were significantly higher in white adipose tissues of *Foxo1*$^{+/-}$ mice (Fig. 4*D*). Quantitative PCR studies also revealed an increase in the expression of *Pck1*, a PPARγ target gene known to regulate glycerogenesis (Fig. 4*E*). Higher Pck1 activity could lead to increased fatty acid reesterification and obesity, consistent with our observed increment in adiposity. We also detected changes in the expression of other PPARγ target genes involved in glucose uptake and oxidation, with increased mRNA levels of *Sorbs1* (also known as *CAP*) and *Pdk4* in HFD-fed *Foxo1*$^{+/-}$ mice (Fig. 4*F*–*G*).

Reduced FoxO1 expression improves the response to PPARγ agonist treatment. The PPARγ nuclear receptor is a well-known molecular target in the treatment of insulin resistance. To further investigate the interaction of FoxO1 and PPARγ in vivo, we treated *Foxo1*$^{+/-}$ and wild-type mice with the PPARγ agonist rosiglitazone. Both groups (4 months old) were fed a 45% HFD with and without rosiglitazone treatment for 4 weeks. Weight gain was identical between genotypes (Fig. 5*A*).

Although FoxO1 haploinsufficient mice showed enhanced insulin sensitivity after 24 weeks of a HFD compared with that of wild-type mice (Fig. 1), both *Foxo1*$^{+/-}$ and wild-type groups were similarly glucose intolerant and insulin resistant after only 4 weeks of a HFD. TZD-treated wild-type and *Foxo1*$^{+/-}$ mice exhibited lower fasting glucose values (Table 1**)** with improved glucose tolerance compared with HFD-fed controls **(**Fig. 5*B***)**. However, TZD-treated *Foxo1*$^{+/-}$ mice demonstrated greater gains in insulin sensitivity with lower glucose excursions after glucose challenge (Fig. 5*B*) and lower basal insulin levels (Table 1) compared with TZD-treated wild-type littermates. Similar results were evident when the decline in glucose levels was measured during an ITT, with greater glucose-lowering effects of insulin in the *Foxo1*$^{+/-}$ mice (Fig. 5*C* and *D*).

The expression of key gluconeogenic genes in liver was measured in both *Foxo1*$^{+/-}$ and wild-type groups after rosiglitazone treatment. TZD-treated *Foxo1*$^{+/-}$ mice showed lower *Pck1* and *G6pc* expression compared with their wild-type controls (Fig. 5*E*), suggesting that decreased gluconeogenesis contributes to the lower glucose values during glucose and insulin tolerance testing. In the liver, the interaction of FoxO1 with PPARγ coactivator 1α (Pgc1α) serves to increase *Pck1* and *G6pc* expression, in cooperation with the cAMP response element-binding protein binding protein coactivator TORC2 (17). Interestingly, TZD-treated *Foxo1*$^{+/-}$ mice showed decreased expression of both *Pgc1a* and *Torc2* (Fig. 5*E*). Lipogenic gene expression (*Scd1*, *Srebp1c*, *Fasn*, and *Acc*) also tended to be lower in fasted liver (Fig. 5*F*), although these differences did not reach statistical significance.

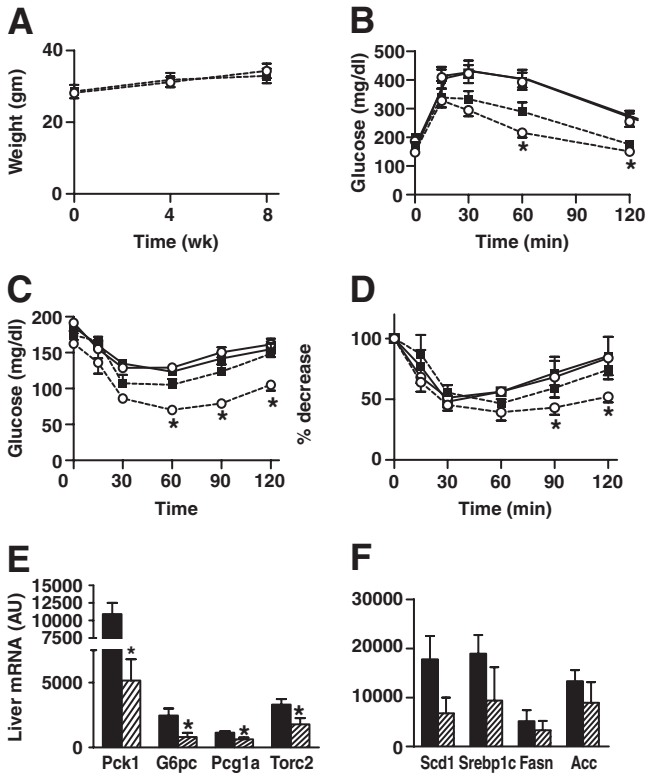

FIG. 5. Effect of TZD treatment on in vivo glucose homeostasis and insulin sensitivity in *Foxo1*$^{+/-}$ mice. *A*: Body weights of male mice were measured at initiation of rosiglitazone treatment and every 4 weeks up to 8 weeks of age (wild-type HFD + TZD $n = 8$; *Foxo1*$^{+/-}$ HFD + TZD $n = 10$). *B*: Glucose tolerance testing (1 g/kg dextrose i.p.) was performed on mice after 5 weeks of combined HFD and TZD (wild-type HFD + TZD $n = 8$; *Foxo1*$^{+/-}$ HFD + TZD $n = 10$) and compared with GTT results from mice after 5 weeks of the HFD alone (wild-type HFD $n = 10$; *Foxo1*$^{+/-}$ HFD $n = 14$). Values represent mean glucose ± SE. *C* and *D*: Insulin tolerance testing (0.35 unit/kg insulin i.p.) was conducted on mice after 5 weeks of combined HFD and TZD (HFD + TZD wild type $n = 8$; HFD *Foxo1*$^{+/-}$ + TZD $n = 10$) and compared with GTT results from mice after 5 weeks of the HFD alone (HFD wild type $n = 10$; HFD *Foxo1*$^{+/-}$ $n = 14$). Results are represented as both absolute glucose values and percent glucose decrease from basal. Glucose curves from both GTT and ITT were significantly different between TZD-treated *Foxo1*$^{+/-}$ and wild-type mice ($P < 0.04$) and between TZD-treated *Foxo1*$^{+/-}$ mice compared with mice fed a HFD alone ($P < 0.001$). ○, HFD *Foxo1*$^{+/-}$; ■, HFD wild type; ○, HFD + TZD *Foxo1*$^{+/-}$; ■, HFD + TZD wild type. *E* and *F*: Liver gene expression studies conducted in TZD-treated *Foxo1*$^{+/-}$ mice used a programmed microarray technique to measure genes that influence both hepatic glucose production and fatty acid synthesis. Relative mRNA values are reported as means ± SE. *$P < 0.05$. AU, arbitrary units. ■, FD + TZD wild type; ▨, HFD + TZD *Foxo1*$^{+/-}$.

Although smaller adipocytes were identified in epididymal fat pads of *Foxo1*$^{+/-}$ mice fed a HFD alone, the opposite was observed in mice after TZD treatment, with a 36% increase in adipocyte size in *Foxo1*$^{+/-}$ mice (Fig. 6*A* and *B*). Adipose tissue macrophages increase in obesity, localizing around adipocytes to form crown-like structures (18). Macrophage infiltration into adipose tissue was attenuated in TZD-treated *Foxo1*$^{+/-}$ mice, with a lower percentage of adipocytes surrounded by MAC2-stained cells (*Foxo1*$^{+/-}$ 2.0 ± 0.7% vs. wild type 2.0 ± 0.7%, $P = 0.07$) and decreased relative expression of F4/80 and CD11c genes (F4/80: *Foxo1*$^{+/-}$ 1.0 ± 0.47 vs. wild type

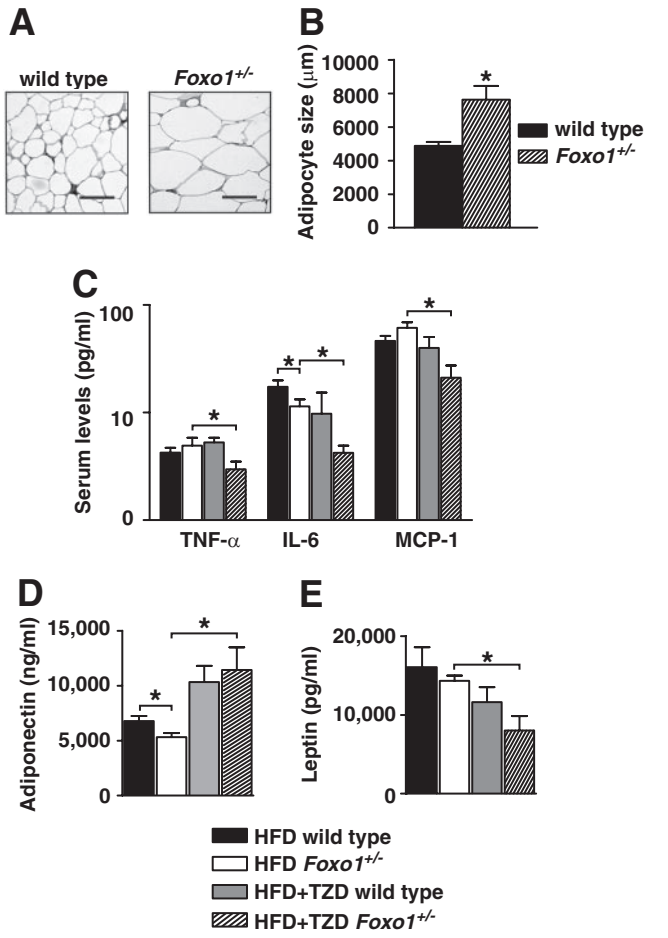

FIG. 6. Cytokine and adipokine profiling in TZD-treated *Foxo1*$^{+/-}$ mice. *A* and *B*: Average size of adipocytes from epididymal fat (wild type n = 4; *Foxo1*$^{+/-}$ n = 5). Representative photomicrographs are represented. Scale bars represent 100 μm. *C–E*. Multiplexed bead immunoassay techniques were used to measure circulating cytokine and adipokine levels in HFD-fed animals in the presence or absence of TZD. Proinflammatory serum cytokines (tumor necrosis factor-α [TNF-α], IL-6, and monocyte chemoattractant protein 1 [MCP-1]) are significantly reduced in TZD-treated *Foxo1*$^{+/-}$ mice. Although serum adiponectin levels are lower in HFD-fed *Foxo1*$^{+/-}$ compared with HFD-fed wild-type, FoxO1 haploinsufficiency is associated with higher elevations in serum adiponectin after TZD treatment. In contrast, serum leptin values decrease to a greater extent in TZD-treated *Foxo1*$^{+/-}$ animals. These serum cytokine and adipokine data are also presented in numeric form in Table 1. Values are reported as means ± SE. *$P < 0.05$. ■, HFD wild type; □, HFD *Foxo1*$^{+/-}$; ▨, HFD + TZD wild type; ▨, HFD + TZD *Foxo1*$^{+/-}$.

6.3 ± 1.9 arbitrary units; CD11c: *Foxo1*$^{+/-}$ 1.0 ± 0.06 vs. wild type 6.3 ± 1.3 arbitrary units; $P < 0.05$).

The enhanced response of *Foxo1*$^{+/-}$ mice to rosiglitazone, as seen by GTT and ITT, was further supported by the TZD-induced decrease in levels of serum cytokines associated with inflammation and insulin resistance (tumor necrosis factor-α, IL-6, and monocyte chemoattractant protein-1) (Fig. 6*C*). PPARγ ligand treatment leads to increased adiponectin and decreased leptin concentrations (19). Although serum adiponectin levels were higher in both genotypes after TZD treatment, *Foxo1*$^{+/-}$ mice showed a greater increment in adiponectin concentration, compared with wild-type littermates (Fig. 6*D*). As expected, serum leptin levels were measurable in HFD-fed wild-type mice. These levels decreased in both groups after TZD administration, consistent with improved insulin sensitivity, although a much greater decrease was observed in *Foxo1*$^{+/-}$ mice (Fig. 6*E*). These data suggest that decreased expression of FoxO1 potentiates TZD action in vivo.

DISCUSSION

FoxO1 transcription factors serve as negative regulators of insulin action, mediating key events in adipogenesis, myogenesis, and glucose homeostasis (20). FoxO proteins localize to the nucleus, where they activate the transcription of target genes. However, upon phosphorylation by Akt, they are exported promptly to the cytoplasm, providing a direct mechanism for insulin-suppressed gene expression (1). Although the FoxO1 isoform has been shown to promote the expression of key gluconeogenic enzymes in liver (12,13,21), it is unclear how it contributes to metabolism in other tissues, particularly adipose and skeletal muscle. In addition, a clear interaction of FoxO1 with the PPARγ nuclear receptor has not yet been demonstrated in vivo. In this study, we show that reduced expression of FoxO1 enhances insulin sensitivity, not only in liver but also in skeletal muscle. In addition, FoxO1 haploinsufficiency is associated with increased expression of PPARγ and PPARγ-dependent target genes in adipose tissue and an improved response to PPARγ agonist treatment during consumption of a HFD.

FoxO1 haploinsufficiency has been shown to attenuate insulin resistance in mice with mutations of the insulin receptor and IRS-2 (3). Here, we demonstrate that FoxO1 heterozygosity confers protection against HFD-induced insulin resistance, despite an increase in epididymal fat mass. Furthermore, our euglycemic clamp studies are the first to measure hepatic glucose output directly in *Foxo1*$^{+/-}$ mice and demonstrate improvements in both basal and insulin-mediated suppression of hepatic glucose production.

In the present study, we noted a decrease in liver size in HFD-fed *Foxo1*$^{+/-}$ mice, with reductions in the hepatic expression of *Scd1*, *Srebp1c*, *Fasn*, and *Acc*, suggesting that FoxO1 promotes fatty acid synthesis in liver. Although we cannot exclude secondary effects due to differences in circulating insulin between genotypes and the presence of relative hyperinsulinemia in HFD-fed wild-type mice, these results are consistent with prior observations linking FoxO1 to insulin-dependent hepatic triglyceride production (21,22) and support the concept that FoxO1 haploinsufficiency may suppress *Srebp1c* and lipogenic gene expression in the liver when insulin signaling is disrupted. Interestingly, prior studies in a transgenic mouse expressing constitutively nuclear FoxO1 in liver showed reduced cholesterol and triglyceride levels with a decrease in lipogenic gene expression (23). This apparent difference may be due to nutrient status, because our *Foxo1*$^{+/-}$ animals were studied while fasting, whereas the constitutively nuclear FoxO1 transgenic mouse was studied after refeeding. Consistent with prior studies in hepatocytes under both in vitro and in vivo conditions, *Pck1* and *G6pc* expression was reduced in *Foxo1*$^{+/-}$ mice.

The FoxO1 isoform is highly expressed in skeletal muscle (3) and has been reported to control myocyte differentiation (24). For example, conditional ablation of FoxO1 in skeletal muscle leads to increased formation of fast-twitch muscle fibers (25), whereas FoxO1 overexpression leads to reduced skeletal muscle mass with a marked decrease in slow-twitch fibers (26). Transgenic FoxO1 overexpression in muscle has also been shown to reduce

skeletal muscle mass with impaired glucose and insulin tolerance (26). Otherwise, little evidence has been reported on the effect of FoxO1 on skeletal muscle metabolism. In this regard, our clamp data show that FoxO1 haploinsufficiency results in significantly improved glucose disposal despite obesity, with a robust increase in insulin-stimulated muscle Akt phosphorylation. Although some effects of FoxO1 may be indirect, these results support the conclusion that FoxO1 plays a regulatory role in skeletal muscle to modulate insulin sensitivity.

Of interest, although many murine models with heterozygous gene deletions do not exhibit a measurable metabolic phenotype, *Foxo1*$^{+/-}$ mice show clear differences in glucose metabolism. In addition, these differences are only apparent in older, obese HFD-fed *Foxo1*$^{+/-}$ mice and not in younger mice or during feeding of normal chow diets. Endogenous FoxO1 is largely dephosphorylated in adipocytes after HFD, remaining localized to the nucleus (27). Thus, the effects of FoxO1 may be greater in HFD-fed animals because dephosphorylated FoxO1 proteins are predominantly nuclear, and, therefore, transcriptionally active. In the *Foxo1*$^{+/-}$ mouse model, improved insulin sensitivity in concert with increased Akt phosphorylation could produce higher levels of FoxO1 phosphorylation, driving FoxO1 nuclear export in a feed-forward manner. In turn, because these mice are haploinsufficient, increased nuclear export of FoxO1 could potentially result in near-complete inactivation of FoxO1, resulting in a phenotype that mimics homozygous deletion of the gene.

FoxO1 is the most abundant FoxO isoform identified in both white and brown adipose tissues (2). Evidence from several laboratories, including ours, suggests that FoxO1 interferes with PPARγ activity in cultured adipocytes. FoxO1 binds to both PPARγ1 and PPARγ2 promoters to repress their transcriptional activity, leading to decreased PPARγ expression (6,7). In addition, we have recently shown that FoxO1 binds directly to PPARγ and disrupts its DNA binding ability (16). Through this mechanism, FoxO1 may interfere with promoter DNA occupancy of the PPARγ receptor.

In this study, we provided additional evidence to suggest that FoxO1 inhibits PPARγ activity in vivo. *Foxo1*$^{+/-}$ mice showed increased PPARγ mRNA in white adipose tissue, suggesting that FoxO1 inhibits PPARγ gene expression. In addition, we measured mRNA levels of several PPARγ target genes and observed enhanced expression of *Pck1*, *Sorbs1*, and *Pdk4*, genes known to participate in glycerogenesis, glucose uptake, and oxidation. Interestingly, FoxO1 has been shown to induce the expression of PDK4 in both skeletal muscle and liver (28), but PDK4 mRNA was enhanced in adipose tissue in FoxO1 haploinsufficient mice in the present study. This increase in adipose *Pdk4* may be secondary to increased PPARγ function with FoxO1 haploinsufficiency, as TZDs have recently been shown to upregulate the expression of *Pdk4* in adipocytes (29). Changes in the activity of PPARγ could account, in part, for the improved insulin sensitivity after feeding of a HFD in *Foxo1*$^{+/-}$ mice.

These findings were further supported by our experiments in TZD-treated animals. Administration of rosiglitazone to obese mice produced significantly greater insulin sensitivity in *Foxo1*$^{+/-}$ mice compared with wild-type littermates. Reduced expression of FoxO1 with subsequent enhancement of PPARγ transactivation could account for this amplified response to the PPARγ agonist.

In conclusion, the present study demonstrates that FoxO1 haploinsufficiency protects against HFD-induced insulin resistance with improvements in both liver and muscle insulin sensitivity. Adipose tissue of *Foxo1*$^{+/-}$ mice also demonstrates increased expression of *Pparγ* and its target genes. Moreover, FoxO1 haploinsufficiency produces an enhanced response to PPARγ agonist treatment. These findings indicate that FoxO1 proteins negatively regulate insulin action in obesity and that their effect may be explained, at least in part, by inhibiting the activation of PPARγ.

ACKNOWLEDGMENTS

This work was supported by National Institutes of Health Grant DK075479.

No potential conflicts of interest relevant to this article were reported.

We thank Mark Schwartz at High Throughput Genomics who performed the programmed array plate gene expression studies. Thanks are due also to Domenico Accili (Columbia University, New York, NY) for helpful discussions and support.

Parts of this study were presented in abstract form at the Keystone Symposium on Type 2 Diabetes and Insulin Resistance, Banff, Alberta, Canada, 20–25 January 2009.

REFERENCES

1. Accili D, Arden KC. FoxOs at the crossroads of cellular metabolism, differentiation, and transformation. Cell 2004;117:421–426
2. Nakae J, Kitamura T, Kitamura Y, Biggs WH 3rd, Arden KC, Accili D. The forkhead transcription factor Foxo1 regulates adipocyte differentiation. Dev Cell 2003;4:119–129
3. Kitamura T, Nakae J, Kitamura Y, Kido Y, Biggs WH 3rd, Wright CV, White MF, Arden KC, Accili D. The forkhead transcription factor Foxo1 links insulin signaling to Pdx1 regulation of pancreatic β cell growth. J Clin Invest 2002;110:1839–1847
4. Spiegelman BM. PPAR-γ: adipogenic regulator and thiazolidinedione receptor. Diabetes 1998;47:507–514
5. Olefsky JM. Treatment of insulin resistance with peroxisome proliferator-activated receptor γ agonists. J Clin Invest 2000;106:467–472
6. Armoni M, Harel C, Karni S, Chen H, Bar-Yoseph F, Ver MR, Quon MJ, Karnieli E. FOXO1 represses peroxisome proliferator-activated receptor-γ1 and -γ2 gene promoters in primary adipocytes: a novel paradigm to increase insulin sensitivity. J Biol Chem 2006;281:19881–19891
7. Dowell P, Otto TC, Adi S, Lane MD. Convergence of peroxisome proliferator-activated receptor γ and Foxo1 signaling pathways. J Biol Chem 2003;278:45485–45491
8. Hosaka T, Biggs WH 3rd, Tieu D, Boyer AD, Varki NM, Cavenee WK, Arden KC. Disruption of forkhead transcription factor (FOXO) family members in mice reveals their functional diversification. Proc Natl Acad Sci USA 2004;101:2975–2980
9. Lesniewski LA, Hosch SE, Neels JG, de Luca C, Pashmforoush M, Lumeng CN, Chiang SH, Scadeng M, Saltiel AR, Olefsky JM. Bone marrow-specific Cap gene deletion protects against high-fat diet-induced insulin resistance. Nat Med 2007;13:455–462
10. Solinas G, Vilcu C, Neels JG, Bandyopadhyay GK, Luo JL, Naugler W, Grivennikov S, Wynshaw-Boris A, Scadeng M, Olefsky JM, Karin M. JNK1 in hematopoietically derived cells contributes to diet-induced inflammation and insulin resistance without affecting obesity. Cell Metab 2007;6:386–397
11. Martel RR, Botros IW, Rounseville MP, Hinton JP, Staples RR, Morales DA, Farmer JB, Seligmann BE. Multiplexed screening assay for mRNA combining nuclease protection with luminescent array detection. Assay Drug Dev Technol 2002;1:61–71
12. Nakae J, Kitamura T, Silver DL, Accili D. The forkhead transcription factor Foxo1 (Fkhr) confers insulin sensitivity onto glucose-6-phosphatase expression. J Clin Invest 2001;108:1359–1367
13. Puigserver P, Rhee J, Donovan J, Walkey CJ, Yoon JC, Oriente F, Kitamura Y, Altomonte J, Dong H, Accili D, Spiegelman BM. Insulin-regulated hepatic gluconeogenesis through FOXO1-PGC-1α interaction. Nature 2003;423:550–555
14. Altomonte J, Richter A, Harbaran S, Suriawinata J, Nakae J, Thung SN, Meseck M, Accili D, Dong H. Inhibition of Foxo1 function is associated

with improved fasting glycemia in diabetic mice. Am J Physiol Endocrinol Metab 2003;285:E718–E728
15. Qiao L, Shao J. SIRT1 regulates adiponectin gene expression through FoxO1-C/enhancer-binding protein α transcriptional complex. J Biol Chem 2006;281:39915–39924
16. Fan W, Imamura T, Sonoda N, Sears DD, Patsouris D, Kim JJ, Olefsky JM. FOXO1 transrepresses PPARγ transactivation, coordinating an insulin-stimulated feed-forward response in adipocytes. J Biol Chem. In press.
17. Koo SH, Flechner L, Qi L, Zhang X, Screaton RA, Jeffries S, Hedrick S, Xu W, Boussouar F, Brindle P, Takemori H, Montminy M. The CREB coactivator TORC2 is a key regulator of fasting glucose metabolism. Nature 2005;437:1109–1111
18. Cinti S, Mitchell G, Barbatelli G, Murano I, Ceresi E, Faloia E, Wang S, Fortier M, Greenberg AS, Obin MS. Adipocyte death defines macrophage localization and function in adipose tissue of obese mice and humans. J Lipid Res 2005;46:2347–2355
19. Johnson JA, Trasino SE, Ferrante AW Jr, Vasselli JR. Prolonged decrease of adipocyte size after rosiglitazone treatment in high- and low-fat-fed rats. Obesity (Silver Spring) 2007;15:2653–2663
20. Accili D. Lilly Lecture 2003: The struggle for mastery in insulin action: from triumvirate to republic. Diabetes 2004;53:1633–1642
21. Matsumoto M, Podai A, Rossetti L, DePinho RA, Accili D. Impaired regulation of hepatic glucose production in mice lacking the forkhead transcription factor Foxo1 in liver. Cell Metab 2007;6:208–216
22. Kamagata A, Qu S, Perdomo G, Su D, Kim DH, Slusher S, Mesenk M, Dong HH. FoxO1 mediates insulin-dependent regulation of hepatic VLDL production in mice. J Clin Invest 2008;118:2347–2364
23. Zhang W, Patil S, Chauhan B, Guo S, Powell DR, Le J, Klotsas A, Matika R, Xiao X, Franks R, Heidenreich KA, Sajan MP, Farese RV, Stolz DB, Tso P, Koo SH, Montminy M, Unterman TG. FoxO1 regulates multiple metabolic pathways in the liver: effects on gluconeogenic, glycolytic, and lipogenic gene expression. J Biol Chem 2006;281:10105–10117
24. Hribal ML, Nakae J, Kitamura T, Shutter JR, Accili D. Regulation of insulin-like growth factor-dependent myoblast differentiation by Foxo forkhead transcription factors. J Cell Biol 2003;162:535–541
25. Kitamura T, Kitamura YI, Funahashi Y, Shawber CJ, Castrillon DH, Kollipara R, DePinho RA, Kitajewski J, Accili D. A Foxo/Notch pathway controls myogenic differentiation and fiber type specification. J Clin Invest 2007;117:2477–2485
26. Kamei Y, Miura S, Suzuki M, Kai Y, Mizukami J, Taniguchi T, Mochida K, Hata T, Matsuda J, Aburatani H, Nishino I, Ezaki O. Skeletal muscle FOXO1 (FKHR) transgenic mice have less skeletal muscle mass, down-regulated type I (slow twitch/red muscle) fiber genes, and impaired glycemic control. J Biol Chem 2004;279:41114–411123
27. Nakae J, Cao Y, Oki M, Orba Y, Sawa H, Kiyonari H, Iskandar K, Suga K, Lombes M, Hayashi Y. Forkhead transcription factor FoxO1 in adipose tissue regulates energy storage and expenditure. Diabetes 2008;57:563–576
28. Barthel A, Schmoll D, Unterman TG. FoxO proteins in insulin action and metabolism. Trends Endocrinol Metab 2005;16:183–189
29. Cadoudal T, Distel E, Durant S, Fouque F, Blouin JM, Collinet M, Bortoli S, Forest C, Benelli C. Pyruvate dehydrogenase kinase 4: regulation by thiazolidinediones and implication in glyceroneogenesis in adipose tissue. Diabetes 2008;57:2272–2279